

RESEARCH

Open Access



Stage-specific impacts of a simulated natural heatwave on *Aedes albopictus*

Claudia Alfaro¹, Alejandro Nabor Lozada-Chávez¹, Ayda Khorramnejad¹, Alida Kropf¹, Paolo Luigi Catapano², Alessia Cappelli², Claudia Damiani², Guido Favia² and Mariangela Bonizzoni^{1*}

Abstract

Background The increase in the frequency and intensity of heatwaves (HWs) under global warming is expected to have more dramatic biological impacts on insects than mean temperature increases. However, evidence of the impact of HWs on insects in their ecological context is limited. Here, we measured across multiple biological scales (e.g., fitness, physiology, transcriptomic and microbiota) the stage-specific responses of the arboviral vector *Aedes albopictus* when experiencing an ecologically relevant HW. In arboviral vectors, only females require a blood-meal thus contributing to the transmission cycle, but other stages can also be the target of vector control strategies. As such understanding the responses to a HW during development has both biological and epidemiological relevance.

Results We observed HW stage-specific responses across the mosquito life cycle. We saw the rate of larvae hatching from eggs exposed to a HW to hatch decreasing and their emergence time increasing. Larvae showed to be resilient to HW by repurposing their energy resulting in trivial mortality. Adults showed sex-specific responses, with extensive male mortality, and a small (16) number of genes elicited following HW exposure, indicating that males are less heat tolerant than females. In females, we observed a reduced reproductive output, only when HW occurred after a blood meal. Finally, we saw extensive HW-dependent changes in the microbial composition of larvae, but female microbiota remained dominated by *Wolbachia* regardless of the thermal challenge.

Conclusions *Ae. albopictus* exhibit stage-specific thermal sensitivities to a HW, which have relevant implications for both the understanding of mosquito biology and the implementation of vector control strategies as the climate crisis progresses.

Keywords Climate change, Fitness, Heatwave, Mosquito, Physiology, Stage-specific

Background

Being dependent on environmental temperature (T_a) to modulate their physiology and behaviour, insects are particularly susceptible to variation in T_a , including both

gradual T_a increase and abrupt T_a shifts to extreme values, broadly defined as coldsnaps or heatwaves (HWs), depending on the direction of the thermal variation with respect to average T_a [1]. Under current global warming, HWs are more prevalent than coldsnaps and increasing in frequency [2]. HW exposure is known to exert profound effects on insects by activating stress response genes (i.e., heat shock proteins, detoxification enzymes and protein kinases) and eliciting thermal tolerance mechanisms, which are energy demanding [3–8]. However, the magnitude of these responses, and consequent fitness costs, are highly variable. They depend not only

*Correspondence:

Mariangela Bonizzoni
mariangela.bonizzoni@unipv.it

¹ Department of Biology and Biotechnology, University of Pavia, Pavia, Italy

² School of Biosciences and Veterinary Medicine, University of Camerino, Camerino, Italy



© The Author(s) 2026. **Open Access** This article is licensed under a Creative Commons Attribution-NonCommercial-NoDerivatives 4.0 International License, which permits any non-commercial use, sharing, distribution and reproduction in any medium or format, as long as you give appropriate credit to the original author(s) and the source, provide a link to the Creative Commons licence, and indicate if you modified the licensed material. You do not have permission under this licence to share adapted material derived from this article or parts of it. The images or other third party material in this article are included in the article's Creative Commons licence, unless indicated otherwise in a credit line to the material. If material is not included in the article's Creative Commons licence and your intended use is not permitted by statutory regulation or exceeds the permitted use, you will need to obtain permission directly from the copyright holder. To view a copy of this licence, visit <http://creativecommons.org/licenses/by-nc-nd/4.0/>.

on HW characteristics, including the level of the thermal shift, its frequency and fluctuating regime, but also on the insect species and its developmental stages [9]. Different instars may have distinct thermal sensitivities, resulting in stage-specific thermal responses [10–12]. As a result, the fitness costs to a HW of the different life-stages of an insect may vary, also in relation to their environment (i.e., aquatic or terrestrial), the accessibility of, and possibility to, move to alternative microclimates, the size of their body and their metabolic state [10, 13, 14]. At present, responses to a HW have been quantified in a limited number of model insect species and often not thoroughly across biological scales, such as fitness, physiology, and transcriptome, thus hindering a comprehensive understanding of the organism's rebound to a hot event [15, 16]. Overall, these knowledge gaps challenge our abilities to predict the impact of future HWs on insects in their different ecological contexts. In mosquito species, which can vector pathogens to humans, assessing the impact of a HW across developmental stages and sexes has both ecological and epidemiological relevance. Only females contribute to the transmission cycle based on their dependency on blood-meals from vertebrate hosts, but control strategies to reduce population size may also target males or eggs and juvenile stages, which occupy different ecological niches than adults [17].

To assess the biological impacts of a HW on mosquitoes, we chose the Asian tiger mosquito *Aedes albopictus*, which is a highly invasive species and the primary vector of arboviruses in temperate areas of the world [18]. Originally from Southeast Asia, *Ae. albopictus* established in Europe and North America in the early 1990s, leading to the emergence of autochthonous arboviral outbreaks [19–21]. We used two populations for which we had previously shown the thermal optimum to be between 23 °C and 26 °C [22] and exposed them to a HW mimicking in a laboratory setting a hot event recorded in the summer of 2021 in Rome [23]. We observed extensive developmental specific-responses, which have relevant implications for both the understanding of mosquito biology and the implementation of vector control strategies as the climate crises progress.

Results

We exposed eggs to hatch, L2 larvae and 5–7-day-old adults of the Foshan and Crema strains to 2 days of 37 °C for 12 h followed by 26 °C for 12 h. In females, we tested the impact of HW in sugar-fed individuals, before and after a blood-meal and their controls (Fig. 1). HW impact was assessed at the fitness, physiological and transcriptomic levels. We further studied HW-related fluctuations in the composition of the microbiota of L2 larvae and sugar-fed females (Fig. 1).

Exposure to a HW during hatching impacts larval viability and hatching time

We observed a significant reduction of larvae emerging from eggs exposed to a HW to hatch in both strains (Fig. 2a; $p < 0.05$ for Crema and $p < 0.01$ for Foshan). Total hatching rate decreased from 98% (± 1) to 55% (± 1) in Crema and from 83% (± 3) to 43% (± 9) in Foshan. To verify if this decrease was due to a halt in hatching during the HW, we followed hatching for 10 days and drew daily hatching rate curves (Fig. 2b). Although larval emergence started to increase 2 days after the HW, it remained lower than that of control mosquitoes for both strains over the course of 10 days. In both strains, we observed no more than 6% hatching during the HW, while the hatching rate of controls reached daily values of 40% and 20% for Crema and Foshan, respectively. Overall, these results indicate that viability of emerging larvae and their emergence time are negatively impacted when eggs are exposed to hatch under a HW.

Larvae are resilient to a HW

We exposed L2 larvae to the HW and tracked their viability and development (Fig. 1). We observed a HW-related mortality of $1.5 \pm 0.06\%$ and $4 \pm 0.68\%$ in Crema and Foshan larvae, respectively (Fig. 2c). Larval viability was significantly ($p = 0.0032$) reduced following HW in Foshan mosquitoes (Fig. 2d). After a HW exposure, larval developmental time of Foshan mosquitoes significantly increased from 12.6 ± 0.1 days to 13.9 ± 0.7 days ($p = 0.04$) (Fig. 2f). A longer developmental time for larvae after HW exposure was also observed in Crema, albeit the difference between HW-exposed and control larvae was not significant (Fig. 2f). We did not observe carry-over effects on pupal developmental time, adult emergence rate and sex ratio (Fig. 2e, g–h).

At the transcriptome level, HW-exposed L2 larvae showed 295 differentially expressed genes (DEGs) with respect to controls (from 18,151 and 18,354 expressed genes detected in control and HW conditions, respectively); 41 DEGs were upregulated and 254 downregulated in exposed larvae vs controls (Fig. 3a, Additional File 1: Table S1). Among the genes that were highly upregulated in exposed larvae, we detected members of the family *protein lethal(2)essential for life* (i.e., LOC109422423, LOC115265018, LOC115265016, LOC109422406, LOC109422446, and LOC109422456) and members of the heat-shock protein (HSP) 70 family (i.e., LOC115265080, LOC109423617, LOC115266509, and LOC115265081) (Fig. 3a), resulting in an enrichment for functions related to protein folding and response to heat (Table 1, Fig. 3d). Among DEGs that were downregulated in HW-exposed larvae, we observed an enrichment

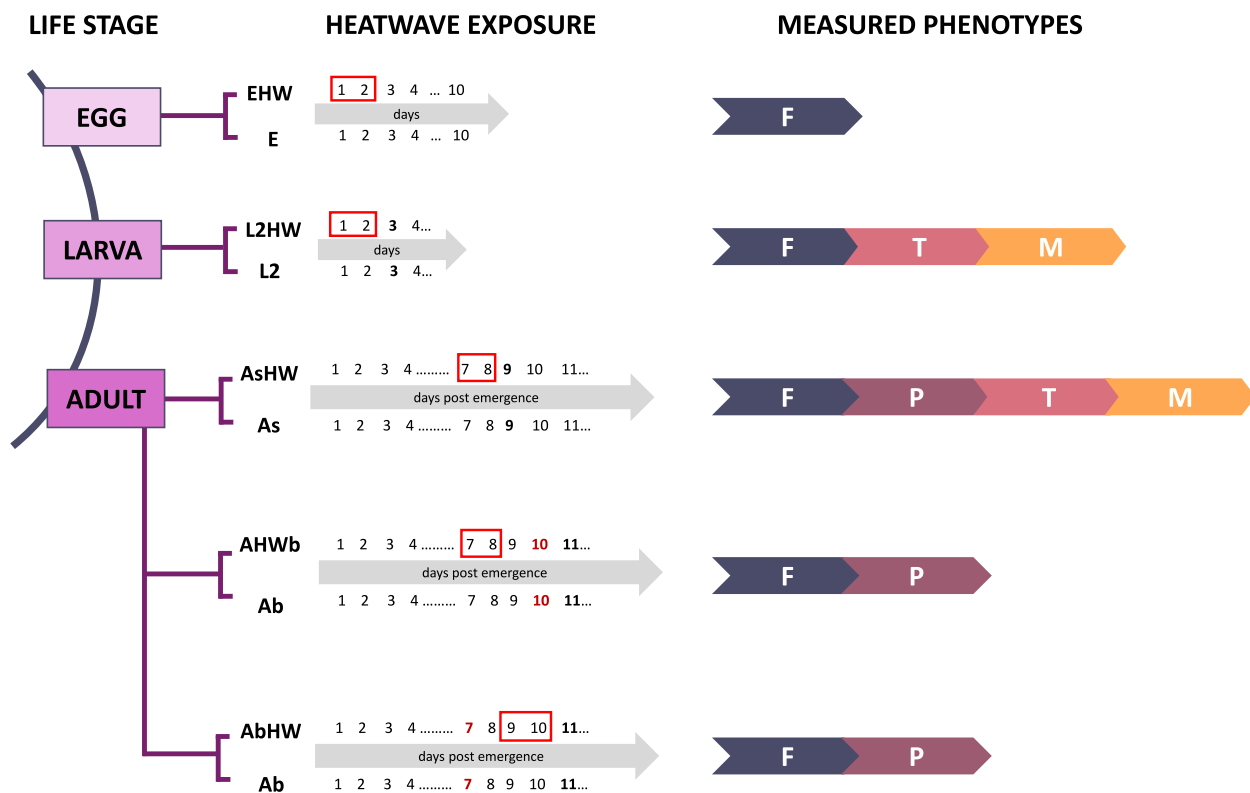


Fig. 1 Experimental design. We exposed to a heatwave (HW, red box) consisting of 2 days at 37 °C for 12 h followed by 26 °C for 12 h, eggs (E), larvae (L2), sugar-fed adults (As) and females offered a blood-meal either before (AbHW) or after (AHWb) the HW. Following the HW and/or the blood-meal, we measured fitness traits (F) and energy reserves (P). For L2 and As samples, we further analysed transcriptional (T) and microbiota (M) changes following a HW. For each treatment, controls were done as indicated in the line below the arrow, which lists the days post emergence. The day in which the blood meal was offered is in red

for genes associated with external encapsulating structures (i.e., LOC109414739, LOC109409014, and LOC109399534), extracellular matrix components (i.e., LOC115262565, LOC115260267, and LOC134287937) and constituents of larval cuticle (i.e., LOC109418197, LOC109413996, LOC115260267, LOC109430468) (Table 1, Fig. 3d). Overall, transcriptomic results suggest that HW-exposed larvae are redirecting energies to thermoregulate and pausing development, which is concordant with the observed delay in their development (Fig. 2f).

Sugar-fed males suffer a higher cost from HW exposure than females

We tested the impact of HW on 5–7-day-old sugar-fed mosquitoes. In both Foshan and Crema, we observed that sugar-fed females suffered low mortality ($3\% \pm 0.49$ in Crema and $8\% \pm 1.19$ in Foshan; Fig. 4a), while more than half of HW-exposed males died ($55\% \pm 4.60$ in Crema and $76\% \pm 16.89$ in Foshan; Fig. 4b). Despite this striking sex difference in the ability to overcome HW exposure, the longevity of Crema mosquitoes surviving HW

exposure did not differ drastically either between sexes or with respect to control mosquitoes (Fig. 4c–d). In contrast, Foshan males that had been exposed to, and had survived the HW, showed a lower survival probability with respect to their control (Mantel-Cox test, $p=0.03$). We further quantified energy reserves in both sugar-fed male and female exposed to a HW with respect to controls. In accordance with longevity data, we saw that males and females differently modulate content of proteins, carbohydrates, glycogen and lipids following a HW (Fig. 4e–l). We observed a significant decrease in protein content in HW-exposed sugar-fed females of both strains ($p<0.0001$ in Crema and $p<0.01$ in Foshan); in males this phenotype was observed only in Crema ($p<0.01$). We further saw that the content of carbohydrates and lipids did not change in males of either strain after HW, but significantly ($p=0.0013$) increased in Crema females (Fig. 4, sections/panels f, h, j, l). The opposite trend was observed in glycogen, which did not change in females, but increased in HW-exposed and surviving males.

At the transcriptome levels, we observed 113 DEGs, 39 upregulated and 74 downregulated in HW-exposed

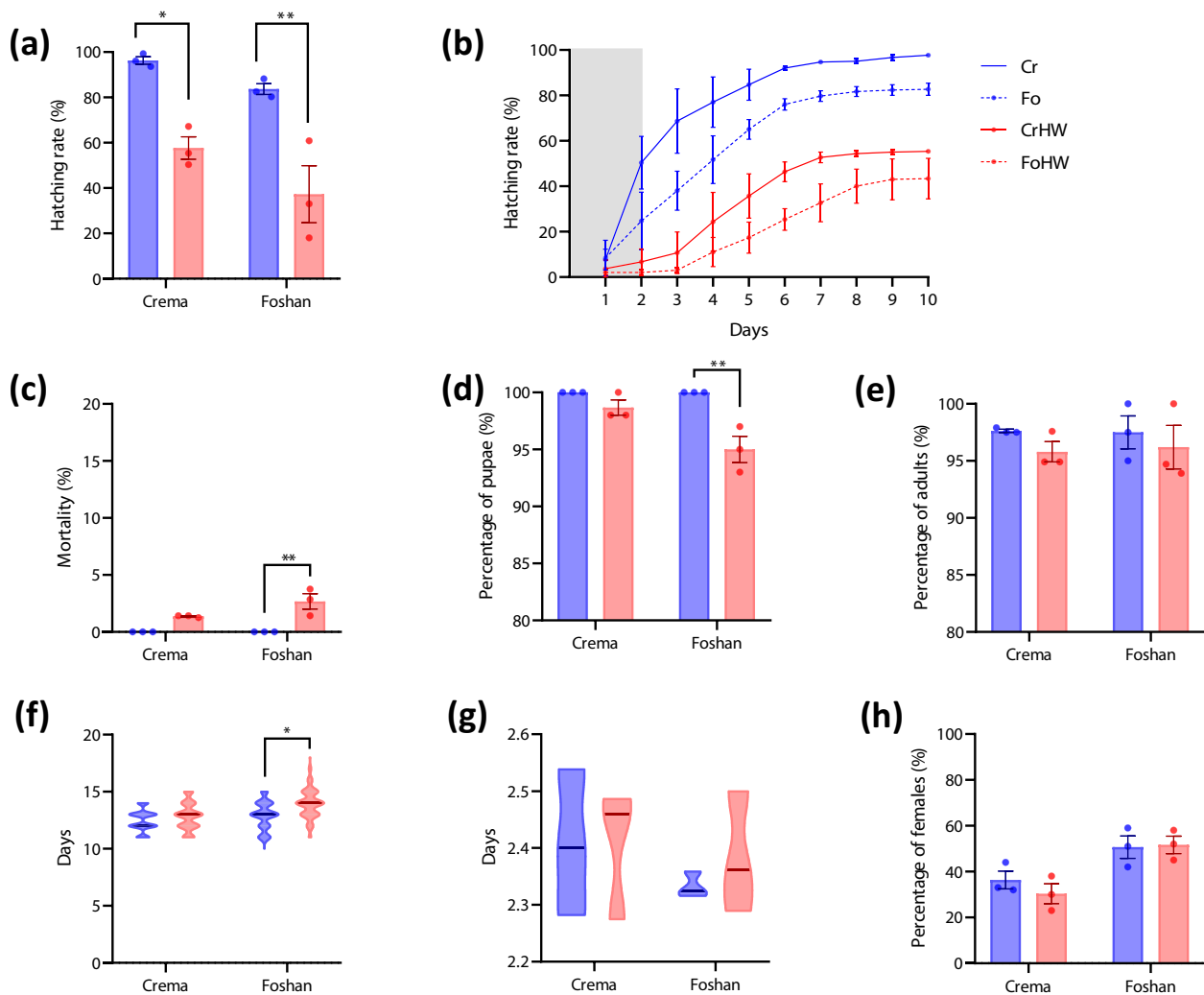


Fig. 2 Effects of HW on eggs exposed to HW to hatch and juvenile stages. **a** Rate of larvae emerging from eggs exposed to a HW to hatch. **b** Percentage of larvae emerging per day from eggs exposed to HW to hatch. Data from Crema (Cr) and Foshan (Fo) mosquitoes are shown with a solid or dotted line, respectively. The grey area marks the 2 days of HW. **c** Mortality of larvae. **d** Larval and **e** pupal viability. **f** Larva to pupa developmental time and **g** pupal developmental time in days. **h** Percentage of emerging females (sex ratio). In all panels, red shows data for HW exposed mosquitoes and blue data of the unexposed counterparts. Statistical differences were tested through a two-way ANOVA. Error bars show the standard error of the mean (SEM). An * refers to a p -value < 0.05, ** to a p -value < 0.01 and **** to a p -value < 0.0001

sugar-fed females vs controls (Fig. 3b, Additional File 1: Table S2, see controls description in Methods section). Among upregulated genes, we detected genes related to several functions such as response to heat (i.e., LOC109422434), oxidative stress (i.e., LOC109408978, LOC109428787, LOC115260130 and LOC134288797), cell metabolism (e.g., LOC109397825 and LOC109417381) and immune response (i.e., LOC134284231 and LOC115256529). However, we could not identify any functional enrichment, probably due to the high percentage (45.1%) of uncharacterized genes (Fig. 3d; Additional File 1: Table S2). On the contrary, downregulated genes were enriched in genes

associated with response to heat (i.e., LOC109422456, LOC109422406, LOC115265016, LOC109422423, LOC115265018 and LOC109422446), protein folding chaperones (i.e., LOC115265081, LOC115266509, LOC115265080 and LOC109423617) and members of the ubiquitin-dependent ERAD pathway (i.e., LOC109413675 and LOC109413676) (Table 1). In males, the number of DEGs was lower with respect to females, with 12 upregulated and 4 downregulated genes in HW-exposed males with respect to controls (Fig. 3c, Additional File 1: Table S2). Among upregulated genes, we observed enrichment for immunity functions (LOC109399074 and LOC134291823) and response to

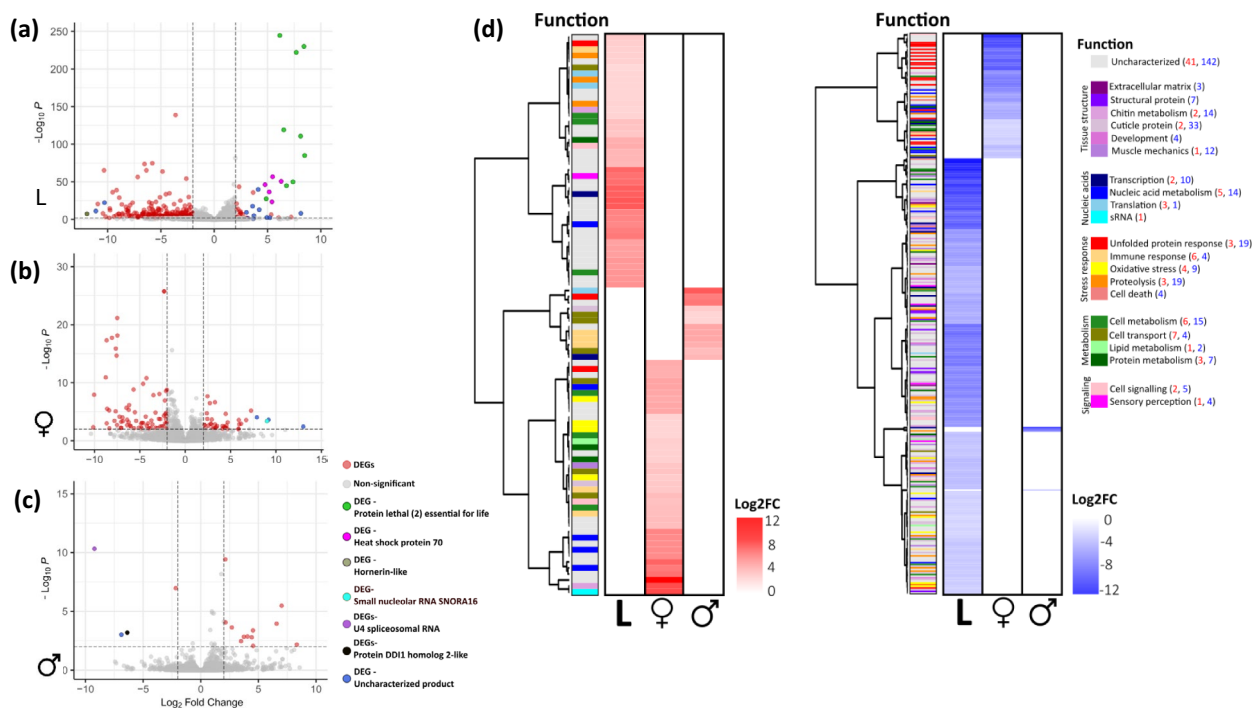


Fig. 3 Transcriptional differences across life stages of the mosquito after a HW exposure. Volcano plots of the differentially expressed genes (DEGs) in **a** larvae (L), **b** females (♀), and **c** males (♂). In all cases, gray dots represent non-differentially expressed genes and red dots show DEGs for comparison between HW-exposed vs control samples. In each panel, dotted lines indicate the thresholds for the p value (<0.01) and the Log_2FC ($<|2|$). Outliers DEGs are coloured based on their function, as described in the legend. **d** Heatmaps showing the upregulated (red) and downregulated (blue) genes in HW-exposed vs control L, female and male samples, along with their function. The numbers in parentheses next to the legend indicate the amount of up (red) or downregulated (blue) genes for each category

stress (LOC109399074 and LOC134291823) (Table 1); while downregulated genes correspond to U4 spliceosomal RNA (LOC115262321), the protein DDI1 homolog 2-like and (LOC134290813) and two uncharacterized genes (LOC134289466 and LOC115262321). Overall fitness, physiological and transcriptomic data, with the number of DEGs in males and their associated functions, support the conclusion that while females are resilient to a HW, males have limited coping mechanisms against a hot event above their thermal optimum.

Exposure to a HW after a blood meal results in reduced fertility

We then proceeded to explore the impact of the HW on the reproductive capacity of males and females. First, we crossed virgin males, which had been exposed and survived the HW, to unexposed virgin females and observed no changes in fecundity and fertility (Fig. 5a–c). Next, we studied the reproductive capacity of females and tested the impact of exposing females to a HW either before or after a blood meal. In females exposed to a HW before the blood meal, we observed a reduction in blood-feeding rate in Crema (two-way ANOVA $p=0.0195$; Fig. 5d), but no significant differences in fecundity and fertility

(Fig. 5e, f). On the contrary, in both strains, we saw a significant reduction of fertility in females exposed to a HW after blood meal (two-way ANOVA, $p<0.001$ in Crema and $p=0.0061$ in Foshan; Fig. 5e, f). Neither females exposed to a HW before or after a blood meal showed changes in sterility rate (Fig. 5g).

Since we did not see significant difference in protein content between blood-fed controls and mosquitoes exposed to a blood meal after HW exposure, we inferred that nutrient from a blood-meal compensate the reduction of protein content as we had observed in sugar-fed mosquitoes exposed to a HW (Fig. 4e). This deduction is further supported by the result shown in Fig. 5j as when mosquitoes are exposed to a HW after having received a blood meal, we see again a reduction of the content of proteins with respect to control blood-fed, but not exposed mosquitoes. In this case the reduction in protein content is lower than what we observed with sugar-fed mosquitoes (Fig. 4e), which is consistent with the hypothesis that nutrients from a blood-meal can compensate for the effects of a HW.

We observed no difference in trypsin-like activity (Fig. 5h) nor protein content (Fig. 5i) between females exposed to a HW before blood meal and their controls.

Table 1 Gene ontology enrichment of DEG after a HW exposure across life stages

GO	ID	Description	Regulation	Gene ratio	Bg Ratio	p adj.	Gene ID
A. Larval stage							
BP	GO:0042026	Protein refolding*	Up	6/36	11/6222	1.82E-09	LOC109422423, LOC115265018, LOC115265016, LOC109422406, LOC109422446, LOC109422456
BP	GO:0009408	Response to heat*	Up	6/36	14/6222	3.89E-09	LOC109422423, LOC115265018, LOC115265016, LOC109422406, LOC109422446, LOC109422456
MF	GO:0044183	Protein folding chaperone	Up	4/59	24/7600	0.00078	LOC115265080, LOC109423617, LOC115266509, LOC115265081
BP	GO:0006950	Response to stress	Down	8/36	297/6222	0.00636	LOC109621883, LOC109418620
CC	GO:0030312	External encapsulating structure	Down	15/76	209/5549	1.47E-06	LOC109414739, LOC109409014, LOC109399534, LOC109404309, LOC109404314, LOC109404300, LOC109404318
CC	GO:0031012	Extracellular matrix	Down	15/76	209/5549	1.47E-06	LOC115262565, LOC115260267, LOC134287937
CC	GO:0005615	Extracellular space	Down	17/76	367/5549	6.33E-05	LOC109400176, LOC109408251, LOC115257192, LOC115257573, LOC109427011, LOC134290023, LOC109396976
MF	GO:0042302	Structural constituent of cuticle	Down	5/59	57/7600	0.00137	LOC109419880
MF	GO:0004252	Serine-type endopeptidase activity	Down	9/59	253/7600	0.00191	LOC109432597, LOC109419403, LOC134285492, LOC109426652, LOC109432998, LOC115253681, LOC134286581, LOC134285010, LOC109418745
MF	GO:0008010	Structural constituent of chitin-based larval cuticle	Down	4/59	45/7600	0.00321	LOC109418197, LOC109413996, LOC115260267, LOC109430468
MF	GO:0030246	Carbohydrate binding	Down	3/59	47/7600	0.04242	LOC134288466, LOC109418338, LOC115268558
B. Females							
BP	GO:0042026	Protein refolding*	Down	6/24	11/6222	8.71E-11	LOC109422456, LOC109422406, LOC115265016, LOC109422423, LOC115265018, LOC109422446
BP	GO:0009408	Response to heat*	Down	6/24	14/6222	1.87E-10	LOC109422456, LOC109422406, LOC115265016, LOC109422423, LOC115265018, LOC109422446
MF	GO:0044183	Protein folding chaperone	Down	6/41	24/7600	6.96E-08	LOC115265081, LOC115266509, LOC115265080, LOC109423617
BP	GO:0030433	Ubiquitin-dependent ERAD pathway	Down	2/24	24/6222	0.03873	LOC109413675, LOC109413676
C. Males							
BP	GO:0006955	Immune response*	Up	2/2	28/6222	2.79E-05	LOC109399074, LOC134291823
BP	GO:0006950	Response to stress*	Up	2/2	297/6222	0.00227	LOC109399074, LOC134291823

*represents a set of genes with two GO terms of equal relevance

We further checked the state of ovaries of females exposed to a HW when maintained under a sugar diet or after a blood meal, since limited availability of proteins can result in ovarian resorption [24]. In both strains, we saw a decrease in protein content in females exposed to a HW after blood meal with respect to control females ($p > 0.05$; Fig. 5j), but this reduction was not as drastic with respect to what we had observed in

sugar-fed females exposed to HW (Fig. 4e). Additionally, we did not see differences in follicle resorption in either sugar-fed females exposed to a HW or in blood-fed females exposed to HW versus control females (Fig. 5k). We observed that eggs of females exposed to a HW before feeding on blood tend to have larger lysosomes than those observed in control females (Additional File 2: Fig. S1), suggesting no resorptions, but alterations of egg physiology.

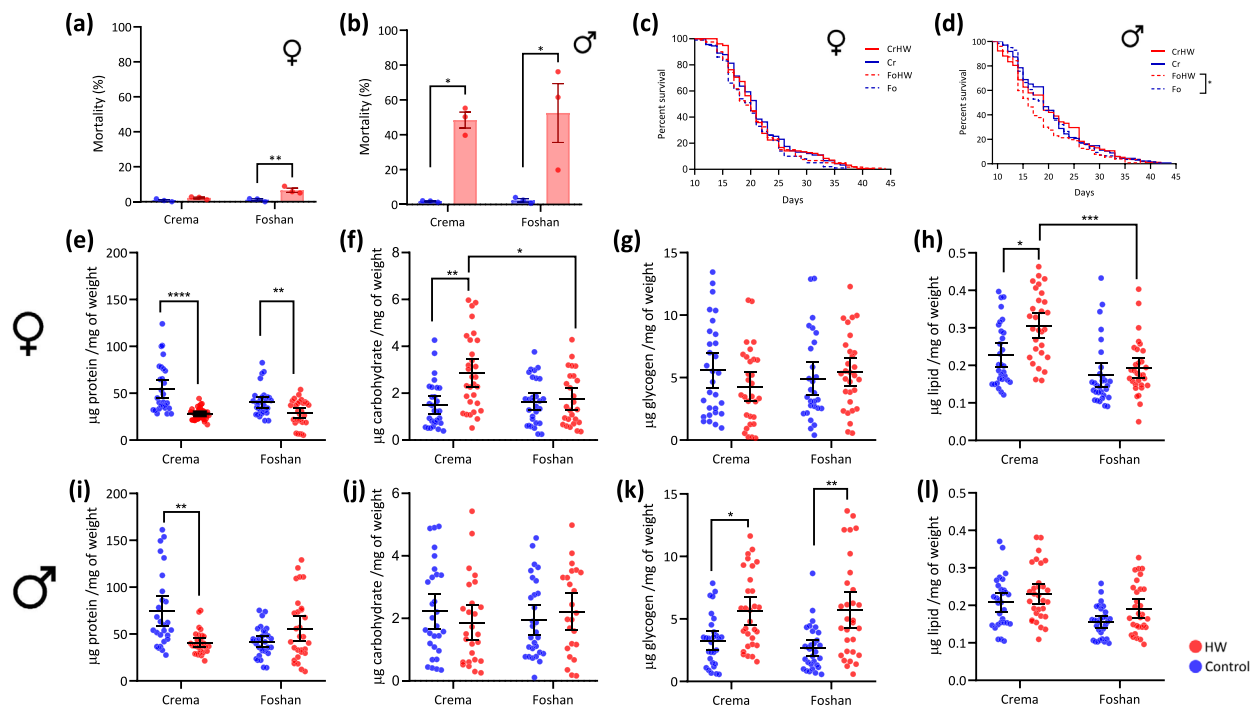


Fig. 4 Effects of a HW in adults. Mortality of females (a) and males (b). Kaplan–Meier survival curves of adults of HW-exposed (red) and control (blue) females (c) and males (d) of Crema (Cr, solid line) or Foshan (Fo, dotted line) strain. Changes in protein (e), carbohydrate (f), glycogen (g) and lipid (h) content in HW-exposed or unexposed females. Changes in protein (i), carbohydrate (j), glycogen (k), and lipid (l) content in HW-exposed and surviving males and their unexposed counterparts. In all cases, red dots show individuals that experienced a HW, whereas blue dots represent those kept at standard rearing conditions (controls). To test for statistical significance, a two-way ANOVA was used for HW-related mortality, a Mantel–Cox test for the survival curves, and a Kruskal–Wallis test for all energetical compartments. Error bars show the SEM. An * refers to a p -value < 0.05, ** to a p -value < 0.01, *** to a p -value < 0.001, and **** to a p -value < 0.0001

HW alters larval but not female composition of the microbiota

Finally, we checked whether HW exposure impacts the composition of the microbiota of L2 larvae and sugar-fed females. In larvae, we identified a total of 29 bacterial taxa (Fig. 6a). We observed that the microbiota of one HW-exposed L2 larval sample of the Crema strain consisted for >90% of *Stenotrophomonas*, a taxon we did not observe in any other sample. To avoid any possible bias, we excluded data from this sample in further analyses. In general, we observed a great variability in the microbiota composition of HW-exposed larval samples with a decrease in *Microbacterium* and *Methylobacterium* and an increase in *Sphingomonas* and *Acinetobacter* in both mosquito populations. We also saw strain-specific blooming of different bacterial taxa, but no changes in *Wolbachia* abundance between exposed larvae and the control samples. Briefly, *Microbacterium* decreased from 32.8–47.3% to 3.3–9.2% in controls vs HW-exposed Crema samples and from 41.1–55.0% to 7.8–21.2% in controls vs HW-exposed Foshan samples (Additional File 1: Table S3); *Methylobacterium* decreased from 1.6–23.6% to 0.2–13.1% in controls

vs HW-exposed Crema samples and from 7.8–21.2% to 2.0–7.0% in controls vs HW-exposed Foshan samples. On the opposite, *Sphingomonas* increased from 0.4–1.7% to 21.1–32.6% in controls vs HW-exposed Crema samples and from 0.3–3.1% to 5.6–24.2% in controls vs HW-exposed Foshan samples and *Acinetobacter* increased from 0.1% to 1.8–25.6% in controls vs HW-exposed Crema samples and from 0.2–0.9% to 1.5–46.6% in controls vs HW-exposed Foshan samples. Strain-specific blooming was observed for *Delftia* and *Chryseobacterium*. *Delftia* increased from 0.0–0.3% to 0.5–2.4% in controls vs HW-exposed Crema samples; while *Chryseobacterium* increased from 0.1–0.5% to 3.2–17.7% in controls vs HW-exposed Foshan samples (Additional File 1: Table S3). *Wolbachia* abundance ranged from 6.7–23.3% to 4.3–23.4% in controls vs HW-exposed Crema samples and from 5.5–13.8% to 5–18.9% in controls vs. HW-exposed Foshan samples. These results were reflected in the beta-diversity analyses, which showed larval samples clustering based on treatment, but not population and unexposed samples having a more homogenous microbiota composition than HW-exposed ones (Fig. 6b). A similar trend

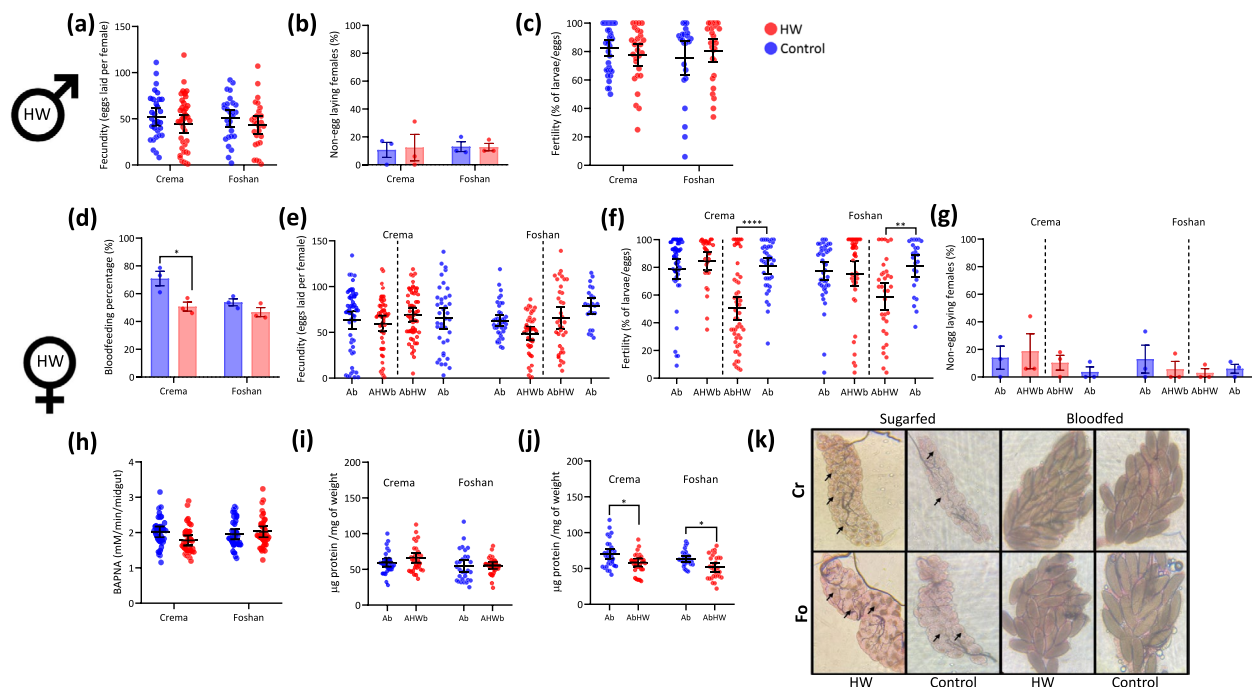


Fig. 5 Reproductive traits of HW survivors. **a** Fecundity, **b** percentage of sterile females, and **c** fertility in virgin females mated with HW-exposed males. **d** Bloodfeeding rate of females exposed to a HW before blood meal. **e** Fecundity, **f** fertility, and **g** percentage of sterile females of females exposed to a HW before (AHWb) and after (AbHW) blood meal. **h** Trypsin-like activity of AHWb 24 h after the bloodmeal. **i** Protein content of AHWb females 3 days post blood meal. **j** Protein content of AbHW immediately after the HW. **k** Ovarian micrographs stained with neutral red of HW-exposed sugar-fed and blood-fed females. Fo and Cr indicate Foshan and Crema mosquitoes, respectively. Arrows indicate the lysosomes in the follicles. In all cases, red and blue dots represent data from HW-exposed or control (Ab) mosquitoes. Control mosquitoes were sampled to be of the same age of HW exposed mosquitoes. Statistical significance was tested using a two-way ANOVA. Error bars show the SEM. An * refers to a p -value < 0.05, ** to a p -value < 0.01, *** to a p -value < 0.001, and **** to a p -value < 0.0001

as described for beta-diversity analyses was observed in the Weighted-UniFrac analysis (Fig. 6c).

The microbiota of sugar-fed female samples was dominated by *Wolbachia*, independently from treatment and population (Fig. 6d). *Wolbachia* ranged from 95.6–100% to 77.9–100% in Crema vs Foshan samples, respectively (Additional File 1: Table S3). As shown by the beta-diversity analyses, the composition, and the relative abundance of bacterial taxa, was overall more homogenous across adults than larval samples and the microbiota of adult samples was also less impacted by HW exposure (Fig. 6e–f).

Discussion

To cope with the thermal stress resulting from exposure to extreme temperatures as during a HW, holometabolous insects may use behavioural thermal regulation strategies like shifting their range and/or may use physiological stage-specific mechanisms that define the thermal sensibilities of each life instar [6]. Here, we show the phenotypic, physiological and transcriptional changes occurring across the development of *Ae. albopictus* when exposed to an ecologically relevant HW, in which the

nightly drop of 11 °C from 37° during the day served as a recovery period [25–27].

We observed that larvae and females are HW resilient, while eggs and males suffer extensive fitness and physiological costs. The rate of larvae emerging from eggs exposed to HW to hatch is consistent with what was reported when hatching *Aedes aegypti* eggs at constant 37 °C [28]. This indicates that hatching occurred both during the hot and the recovery periods of our HW regime. However, the fact that the rate of larvae emerging from eggs exposed to HW to hatch was lower than that of the control suggests embryo or emerging larvae mortality due to elevated temperature. Aquatic larvae are expected to be sensitive to heat [6], but our results showed that mosquito larvae can overcome HW exposure by delaying their development. The hypothesis of larval developmental delay is supported by our transcriptional data, which showed lower expression of growth-related genes (i.e., *apnoia* and *agrln*), multiple cuticle and chitin-related genes, genes encoding for muscle-related proteins (e.g., *titin*) and genes involved in cornification (i.e., *hornerin-like* and *loricrin*) in HW-exposed larvae with respect to unexposed larvae. In *Ae. aegypti*, the heat response of

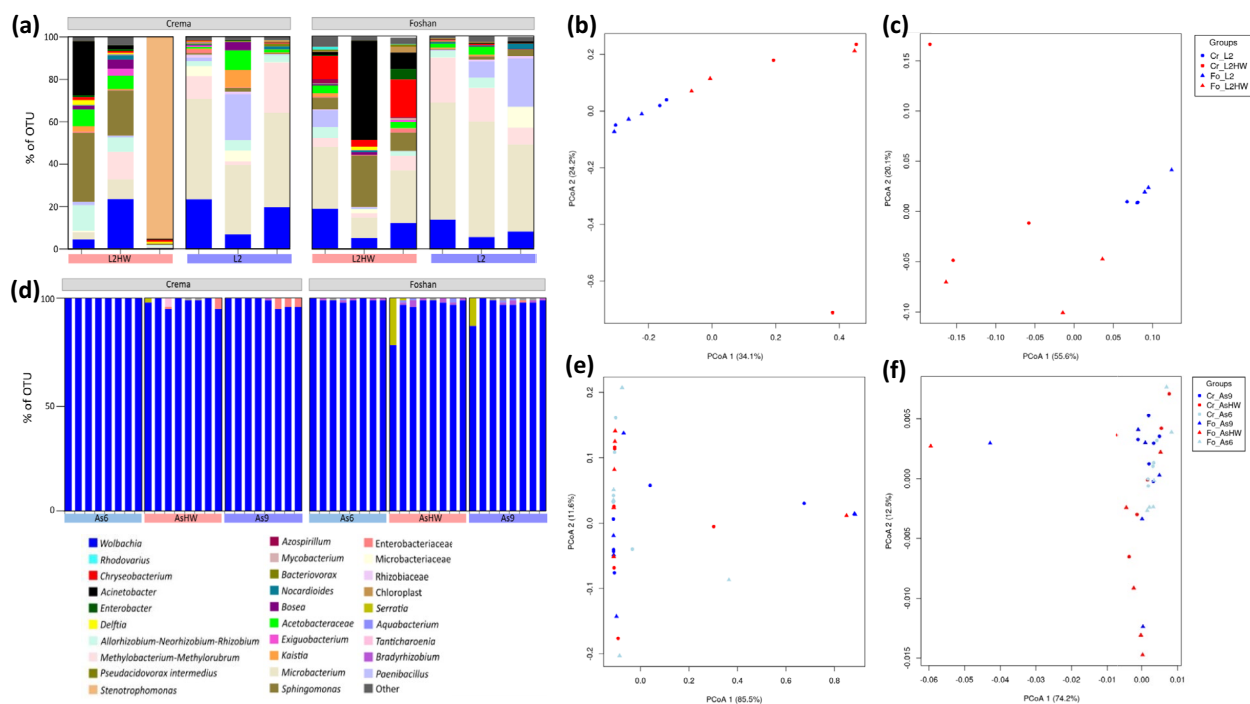


Fig. 6 Changes in bacterial composition after a HW. **a** Barplot of bacterial taxa in HW-exposed L2 larvae (L2HW) and unexposed samples (L2). Brays-Curtis and Weighted-UniFrac analyses of larvae (**b**, **c**), respectively. **d** Barplot of bacterial taxa of unexposed and HW-exposed samples, with their respective Bray–Curtis (**e**) and Weighted-UniFrac analyses (**f**). In each panel, data for Foshan (Fo) or Crema (Cr) mosquitoes are in triangle or circle, respectively. Red shows data from HW-exposed samples, blue to data of control samples. For females, we collected unexposed control samples at 6 (As6, light blue) and 9 (As9, dark blue) days post-emergence to match the age before and after HW-exposed samples (AsHW)

larvae is very dynamic, with a higher HSP expression than in other life stages [29]. We also found that the highest number of HSPs was elicited in larvae than in adults following HW exposure. Upregulated HSPs included members of the *protein lethal(2)essential for life*, which belong to the family of *hsp20*, and members from the *hsp70* family. Both families of chaperones are known to contribute to thermal tolerance in insects [30].

At the adult stage, we observed extensive sex-differences in response to HW exposure. We saw that males surviving HW-exposure accumulated glycogen. Glycogen is mainly used to fuel short-term flight in insects; its increase suggests males reduce movement during HW [31], which can limit their range shifts to more favorable microclimates. In accordance with this hypothesis, we saw more than 50% male mortality following HW exposure supporting the conclusion that HWs can be a strong selective pressure for males, ultimately impacting mosquito population size. At the transcriptome level, males surviving HW exposure upregulated mostly immunity genes such as the antimicrobial peptides defensin A, B, and C. Defensins are elicited upon tissue damage to prevent infections [32], supporting the hypothesis of heat-induced tissue damage in males. Differently than males,

females showed less than 20% HW-related mortality and extensive transcriptional responses. We found several members of the *hsp70* (i.e., *heat shock protein 70 B2*, *heat shock protein A1-like*, *heat shock protein 70 A1*) and *hsp20* (i.e., *protein lethal(2)essential for life*, *protein lethal(2)essential for life-like*) families, which are upregulated in HW-exposed L2 larvae, being downregulated in HW-exposed females, further highlighting the stage-specificity of these proteins. Expression of HSPs is dynamic and dependent both on the length and intensity of the thermal challenge [6] because a high expression of HSPs is costly and may interfere with several cellular processes resulting in toxicity [33]. Downregulation of *hsp70* and *protein lethal(2)essential for life* in females following HW exposure may impact their vector competence as the replication of both Zika and dengue viruses is positively regulated by *hsp70* [34, 35]. While, we saw only one member of the *hsp20*, a *protein lethal(2)essential for life* (i.e., LOC109422434) being upregulated in sugar-fed females exposed to a HW, we found several genes involved in oxidative stress (i.e., *Senecionine N-oxygenase*, *farnesol dehydrogenase-like*, *NADH-ubiquinone oxidoreductase chain 2-like*, *estradiol 17-beta-dehydrogenase 11-like*) and genes involved in cell metabolism (i.e., *alkaline phosphatase*

4-like, regucalcin, max-like protein_X) being highly (>2 LogFC) upregulated in sugar-fed HW-exposed females, which agrees with the observed higher abundance in lipids and carbohydrates. These results suggest that females can tolerate a HW by increasing their sugar and lipid metabolism resulting in production of free radicals, which require activation of detoxification mechanisms [6].

Results from investigations testing the impact of hot treatments designed with no recovery periods show extensive negative effects on the reproductive output of various insect species including *Dr. melanogaster* and other Drosophilidae, the red flour beetle *Tribolium castaneum*, the bed bug *Cimex lectularius*, the parasitoid *Aphidius avenae* and the oriental fruit moth *Graphilota molesta* through alterations of insect behaviours and gamete production and viability [36–42]. We saw a reduction of female fertility when HW exposure occurred immediately after the blood-meal, but we did not see a reduction in either fecundity or fertility in HW-exposed males or females exposed to HW before the blood-meal. Biological effects of a hot event depend on a subtle balance between heat stress related injuries and the possibility to recover during fluctuations to milder temperatures [27]. Thus, the nightly recovery period of our HW regime could have buffered the heat-related injuries from exposure to 37 °C, a temperature close to the *Ae. albopictus* physiological threshold [22]. Additionally, we exposed to the HW sexually mature mosquitoes, which, in the case of males, were allowed to mate for 5 days after HW exposure. We cannot exclude that potential negative HW impacts were masked by a compensatory effect in the days following the HW as male insect fertility appears to be mostly impacted when the hot event occurs before sexual maturation [36]. While we recognize that additional studies mostly exposing males at emergence and restricting their mating window, in addition to experiments testing alternative HW regimes should be explored to further understand the biological impact of hot events on *Ae. albopictus*, we highlight the ecological relevance of our results. Italian meteorological records show the frequent occurrence of hot events, mostly consisting of 2 to 3 days with a thermal maximum in the range of 37–38 °C followed by 24–27 °C at night in the summer months for the past decade [43]. These thermal conditions are very similar to our HW, with the difference that in the laboratory shifts from daily to nightly temperatures are more rapid (approximately 40 min) with respect natural day-night switches. Additionally, despite Foshan and Crema mosquitoes being genetically different and having a different thermal optimum [22], their developmental-specific responses to our HW regime were mostly concordant, allowing for generalization. Our

findings have thus important implications for predicting mosquito population dynamics under current global climate changes and organize control strategies. Our results indicate that control of juvenile stages would be effective through the summer season as larvae appear to be heat resilient and their development may lengthen in response to hot events. At the same time, the observation of a decrease in *Microbacterium* in HW-exposed L2 larvae provide indication on insecticide choices as *Microbacterium* is among the insect gut bacteria shown to be able to degrade pyrethroid and organophosphate insecticides [44]. Our results on the vulnerability of males to a HW highlight the importance of programming releases of gamma rays and X-rays sterile males used in sterile insect technique (SIT)-based strategies and males carrying a dominant lethal gene (i.e., release of insects carrying a dominant lethal, RIDL) [45, 46] in relation to weather forecast to possibly avoid hot events that could decrease the efficacy of male releases. Our data on female resilience to HWs and the absence of HW-dependent fluctuations of *Wolbachia* in sugar-fed females exposed to a HW are consistent with previous studies showing that the wAlbB strain, both in its native and transinfected hosts, is resilient to heat stress. These results are ecologically valuable as they reflect the phenotypic stability of *Wolbachia* within its native host after thermal stress. Such stability could influence subtle gradients in reproductive distortion due to natural fluctuations in native *Wolbachia* density [47, 48].

Conclusions

We show that *Ae. albopictus* mosquitoes respond differently to an ecologically relevant HW depending on their developmental stage and sex. Our findings underscore how thermal vulnerability aligns with biological responses, for instance males exhibited a limited stress response that correlates with their high mortality when exposed to HW, and emphasize the importance of considering full life cycles when predicting mosquito population dynamics and organizing intervention strategies. As ecological models and vector control programs are incorporating climate variability, a mechanistic and stage-specific understanding of HW responses will be essential for accurate predictions and effective interventions.

Methods

Mosquitoes

We used *Ae. albopictus* of the genome-reference Foshan strain [49], along with mosquitoes adapted to the laboratory from eggs collected in the city of Crema in Italy in 2017 [22]. Since laboratory adaptation, both strains have been maintained in Binder KBWF climatic chambers under standard rearing conditions of 12 h at

28 °C and 12 h at 26 °C (light:dark), with 70% relative humidity. We rear larvae in BugDorm plastic containers (19×19×16 cm) at a density of 200 larvae for 1 L of water. Food is provided daily in the form of fish food (Tetra Goldfish Gold Colour). Adults are kept in BugDorm cages (32.5×32.5×32.5 cm) and fed with cotton soaked in 20% sugar solution. Each cage contained approximately 150 adults. Females were bloodfed with commercial defibrinated mutton blood (Biolife Italiana) using a Hemotek blood membrane feeding apparatus.

Heatwave

Using a Binder KBWF, we mimicked a HW that lasted 2 days and consisted of a cycle of 12 h at 37 °C, followed by 12 h at 26 °C (light:dark, 70% relative humidity) (Additional File 3: Fig. S2a). After HW exposure, mosquitoes were moved back to standard rearing conditions.

Assessment of fitness traits

For each strain, we measured: rate of larvae emerging from eggs exposed to HW to hatch, larval viability and larval developmental time, pupae viability and pupae developmental time, female and male longevity of virgin mosquitoes, and their reproductive capacity. We describe below how each fitness parameter was measured.

Larvae emerging from eggs exposed to HW to hatch

For each strain, three groups of 350 eggs were hatched in plastic containers (19×19×16 cm) with 1L of water at 37 °C and immediately placed into the Binder KBWF set to the HW regime. After the HW, trays were moved to standard rearing conditions. In parallel, three groups of 350 eggs were hatched in 1L of water at 28 °C and kept under standard rearing conditions. To avoid any age bias in the experiment, eggs exposed to HW and their controls were from the same generation. Eggs had been stored at 28 °C for 3 days prior to hatching. For each tray, we counted larvae that hatched daily for 10 days. Emerging larvae were removed from each tray to avoid counting errors. The percentage of emerging larvae with respect to the initial number of eggs was used as a measure of hatching rate.

Larvae and pupae fitness parameters

For both strains, we exposed a total of 210 L2 larvae to our HW. After HW exposure, we counted the number of dead larvae to assess HW-related mortality. We transferred survivors to the standard regime and tracked their growth daily to measure larval developmental time as the number of days it took until pupation, larval viability as the percentage of pupae with respect to initial larvae, pupal developmental time as the time of adult emergence from pupae and pupal viability. Finally, we calculated the

sex ratio counting the number of females and males that emerged.

Adult fitness parameters

For adult traits, three biological replicates were performed. Each biological replicate consisted of three BugDorm Cages (W32.5×D32.5×H32.5 cm) containing 80 adults each, giving a total of 240 adults per replicate. Experiments were conducted in parallel for both strains. We used BugDorm Cages made of nylon mesh to guarantee uniform temperature and humidity as set in the climatic chamber. For each replicate, we randomly sampled from the three cages/populations around 80, 5–7-day-old individuals of each sex, exposed them to the HW, counted the number of dead adults immediately after HW exposure and sex-sorted the surviving adults to follow females and male longevity, separately. From the same three cages/replicate, we also sampled males and females to test their reproductive capacity. For males, between 11 and 12 males/strain/replicate surviving HW exposure were allowed to mate with unexposed virgin females. We set up a total of seven crosses following a ratio of 1 male:4 females in groups of 5 males per cage. After 7 days, we offered a blood meal, and randomly sampled 12 engorged females per replicate, which were gently transferred to a cage to individually measure both their fecundity and fertility [50]. We further confirmed the mating status of females that had not deposited eggs by dissecting and viewing their spermatheca under an Olympus CKX53 microscope. For females, we tested their reproductive capacity exposing them to HW either before or after the blood meal. In the former, 18 females per biological replicate were randomly sampled and allowed to recover from the HW for 24 h before offering a blood meal; we also counted the number of females acquiring a blood meal to check if blood feeding rate is affected by HW exposure. In the second scenario, that is exposure to HW after the blood meal, we offered a blood meal to 5–7-day-old females and randomly sampled 16 fully engorged females per biological replicate and waited 24 h before exposing them to the HW. For both scenarios, we had a group of control mosquitoes maintained under standard conditions. In all cases, fecundity and fertility was measured under standard conditions.

Energy reserves quantification

We quantified protein, carbohydrate, glycogen and lipid content using a colorimetric assay as previously described [22] in 30 males and 30 sugar-fed females after HW exposure and their respective controls. Adults were 5–7 days old when they were exposed to the HW. We further quantified protein content in 30 females that had taken a blood meal followed by HW exposure

and their respective controls. We weighed individuals using a microbalance (Mettler AC100). Then, using pestles we homogenized samples individually in 180 μ L of lysis buffer (100 mM KH_2PO_4 (Sigma-Aldrich), 1 mM DTT, 1 mM EDTA (ThermoFisher) pH 7.4) and measured absorbance using a CLARIOstar plate reader (BMG Labtech).

Midgut trypsin-like activity

One day after females surviving the HW took a blood meal, we measured their midgut trypsin-like activity. On ice, we dissected midguts of at least 36 females per strain and tested trypsin enzymatic activity as previously done [51]. Briefly, we used pestles to homogenize each sample in 100 μ L extraction buffer (20 mM Tris/20 mM CaCl_2 (Sigma-Aldrich), pH 8). Then, we centrifuged samples for 2 min at 14,000 g at 4 $^\circ\text{C}$, we collected the supernatants and stored them at -80 $^\circ\text{C}$ until measurements. We added 5 μ L of each sample to 100 μ L of $\text{N}\alpha$ Benzoyl-L-Arginine-p-Nitroanilide (BAPNA; Sigma-Aldrich) in a 96-well plate, which were then incubated at 37 $^\circ\text{C}$ for 10 min. We read the absorbance at 405 nm using a CLARIOstar plate reader (BMG Labtech). We quantified trypsin-like activity using 20 μ g of trypsin from Bovine Serum (Sigma-Aldrich) for the standards.

Microscopy analyses of ovaries

From each strain, we collected 10 sugar-fed females and 10 females that had been offered a blood meal before HW exposure and we examined ovary resorption immediately after HW as described by Clifton & Noriega [52]. Briefly, we dissected ovaries and rinsed them in physiological saline buffer (APS; MgCl_2 0.6 mM, KCl 4 mM, NaHCO_3 1.8 mM, NaCl 150 mM, HEPES 25 mM, CaCl_2 1.7 mM (all Sigma-Aldrich)). Afterwards, we stained ovaries with 0.5% neutral red solution (Sigma-Aldrich) in acetate buffer pH 5.2 (Sigma-Aldrich) for 10 s, rinsed them again in APS and placed them under a coverslip. We visualized samples using an Olympus CKX53 microscope.

Transcriptome analyses

We collected three pools of 10 L2 larvae of the Crema strain immediately after HW and three pools of 10 L2 larvae kept at standard rearing conditions as control. We also sampled four Crema females and four Crema males 24 h before HW (i.e., 6 days old), and immediately after HW exposure. We additionally collected the same number of females and males that had been kept at standard rearing conditions (i.e., control conditions) for the period at which the other experimental group had been exposed to the HW (i.e., 9 days old) (Additional File 3: Fig. S2). We dissected the abdomens of each adult. Larval pools and individual abdomens were homogenized in 50 μ L

of TRIzol (Life Technologies) and stored at -80 $^\circ\text{C}$ until extraction. We performed RNA extraction following the standard TRIzol procedure and re-suspended samples in a final volume of 20 μ L of nuclease-free water. We sent total RNA to BGI Hong Kong for quality control, TruSeq-Stranded mRNA library preparation and sequencing on the Illumina platform. Libraries were sequenced pair-end (2 \times 100 bp) at a depth of 30 million reads.

For RNAseq analysis we used the nf-core/RNAseq pipeline v3.17.0 [53] with the latest AalbF5 genome assembly of *Ae. albopictus* (RefSeq: GCF_035046485.1). The pipeline includes quality check of reads and their trimming before genome mapping for gene expression quantification. We included sequence reads corrections in our nf-core/RNAseq command line for salmon to prevent a “random hexamer priming bias” and a “GC bias,” as suggested [54, 55]. We used fragments per kilobase of exon per million mapped reads (FPKM) to quantify gene expression (Additional File 1: Table S4). First, we defined a gene as expressed when the gene reads counts $\neq 0$, which allowed us to estimate the total fraction of genes expressed under a HW across the AalbF5 whole genome for different life stages (Additional File 1: Table S5). Overall, in the larval samples, we detected a total of 18,151 expressed protein-coding genes in the control conditions, while a total of 18,354 expressed protein coding genes in samples exposed to the HW, which accounts for 76.80% and 77.66% of the AalbF5 proteome, respectively (Additional File 1: Table S5). In samples from adult females, we detected 18,610 expressed protein-coding genes under control conditions and a total of 18,376 expressed protein coding genes in samples that had been exposed to the HW, which represent 78.74% and 77.75% of the AalbF5 proteome, respectively. Finally, in males we detected 18,916 and 19,090 expressed protein-coding genes in control samples and samples exposed to the HW, respectively. This represents 80.03% and 80.77% of the AalbF5 proteome, respectively. Second, we performed a Principal Component Analysis (PCA) with RStudio v4.4.1 to show the association between samples based on the raw reads counts and developmental stage, sex and treatment (Additional File 4: Fig. S3a). Third, we compared gene expression across conditions and life stages using the DeSeq2 package v1.46.0 in R studio [56] and defined differentially expressed genes (DEGs), when $|\text{Log}_2\text{Fold change (FC)}| \geq 2$ and a p -value ≤ 0.01 . We evaluated a filter-bias DEGs detection by performing a linear regression between Log_2FC value thresholds (1, 1.5, and 2) against the total number of DEGs detected in all thresholds. This analysis was performed for larvae, females and males separately (Additional File 4: Fig. S3b). A fit linear model was obtained across the DEGs and the thresholds using the “trendline” feature of Microsoft Excel v. 2503,

compilation 16.0.18623.20116, 64-bits (Microsoft Corporation 2024). A linear correlation between the total DEGs and Log_2FC thresholds was interpreted as the lack of any bias imposed by the selected parameters, that is (1) a decrease in the total DEGs when the threshold stringency increased and (2) no major variation of the total DEGs, even with the highest threshold value. To identify DEGs associated with HW-exposure in larvae, we performed pairwise comparisons between HW-exposed samples and samples maintained under standard conditions (Additional File 1: Table S1) [57]. For adults, since the HW lasts 2 days, we first verified any possible bias due to mosquito aging. We identified DEGs between 6-day-old adults without any exposition and HW-exposed adults (List A, 158 genes), between 6-day-old and 9-day-old unexposed samples (List B, 99 DEGs) and between 9-day-old unexposed controls and HW-exposed samples (List C, 113 DEGs) (Additional File 1: Table S2; Additional File 3: Fig. S2b). We reasoned that List B contains DEGs attributable only to age differences, while Lists A and C contain DEGs that might be affected either by both age and HW, or just one of them. If our HW regime were to induce quiescence, we would expect the transcriptome of HW-exposed adult samples to be more like that of 6-day-old adults rather than that of 9-day-old unexposed controls. However, List A (DEGs between 6-day-old adults and HW-exposed adults) includes 158 DEGs, only 13 of which are shared with List B (DEGs between 6-day-old and 9-day-old unexposed adults). On this basis, we conclude that it is very unlikely that our HW regime halted development. Therefore, we focused on DEGs of List C (9-day-old unexposed adults vs HW-exposed adults) to understand the impact of HW on the transcriptome of adults (Additional File 1: Table S2). The distribution and the statistical significance of DEGs exposed to a HW were shown in volcano plots, using the R package EnhancedVolcano v1.24.0 [58]. To identify genes that significantly deviate from an expected distribution, suggesting highly expressed genes, we identified outliers across each DEGs distribution in larvae, females and males, using a two-sided interquartile range test [59].

Functional gene annotation and gene enrichment analysis

We extracted gene functions of the DEGs of the three above-described lists from the reference genome AalbF5, followed by manual comparison of the gene functions, as well as a GO enrichment analysis (Additional File 1: Table S6). As shown in Additional File 3: Fig. S2b, we used only the DEGs present in List C for further analysis. GO functional gene assignment and gene enrichment were carried out with RStudio v.4.4.1 based on developmental stage, sex, and treatment. We performed GO functional gene assignment and gene enrichment analysis

as described by Lozada-Chávez et al. [60]. Briefly, we generated an annotation database of the AalbF5 genome assembly from results of three approaches, which were merged with Blast2GO [61]. The three approaches are: (1) GO annotations spanning around 72% of 20,424 protein coding genes of the AalbF5-proteome (RefSeq accession number GCF_035046485.1) obtained from NCBI RefSeq database [62]; (2) a BLAST search of homologs of the AalbF5-proteome against the NCBI Diptera nr database v5; (3) a search of functional orthologs with InterProScan v5 [63] against the protein-domain databases Pfam v33.1 [64], ProSiteProfiles v20.2 [65], SUPERFAMILY v2.0 [66] and TIGRfam v15.0 [67]. From this approach, we annotated 82% of the AalbF5-proteome. Then, we performed the GO enrichment analyses using our in-house R-package org.Aalbopictus.eg.db (merged GO annotations) with clusterProfiler v4.2.2 [68]. We corrected the obtained p -values ($p < 0.05$) for multiple tests using the Benjamini–Hochberg procedure, and we removed the redundancy of enriched GO terms for each major GO classification using the function simplify, both included in clusterProfiler.

Microbiota analysis

We sampled three pools of 10 L2 larvae immediately after HW exposure and the same number of larvae maintained under standard conditions as control. We also collected eight sugar-fed females after HW exposure or, as control, eight sugar-fed females not exposed to the HW and of the same age as those HW-exposed. We sterilized all samples by rinsing them in a 2% sodium hypochlorite solution for 10 min, followed by surface disinfection for 5 min with $1 \times$ phosphate buffered saline (PBS), 70% ethanol for 2 min and two more rinsings with sterile water. Afterwards, we dissected the abdomens of each female. We used the Wizard[®] Genomic DNA Purification Kit (Promega) for DNA extraction of larval pools and single abdomens following the manufacturer's instructions. We resuspended DNA in 20 μL nuclease-free water. Samples were analysed through next-generation sequencing (NGS) using a bacterial 16S rRNA gene target. NGS experiments were conducted by Genomix4life S.R.L. (Baronissi, Salerno, Italy). We assessed DNA quality using a NanoDrop One spectrophotometer (Thermo Scientific, Waltham, MA) and a Qubit Fluorometer 4.0 (Invitrogen, Carlsbad, CA). Library preparation targeted the hypervariable V3–V4 region of the 16S rRNA gene using the oligonucleotides 16S Amplicon PCR F (5'-TCGTCCGGCAGCGTCAGATGTGTATAAGAGA CAGCCTACGGGNGGCWGCAG-3') and 16S Amplicon PCR R (5'-GTCTCGTGGGCTCGGAGATGTGTA TAAGAGACAGGACTACHVGGGTATCTAATCC-3') [69]. We assembled each PCR reaction according to the

Metagenomic Sequencing Library Preparation protocol (Illumina, San Diego, CA). A negative control was included in the workflow, consisting of all reagents used during sample processing (16S amplification and library preparation) but without template DNA, to ensure the absence of contamination. We quantified the libraries using a Qubit fluorometer (Invitrogen, Carlsbad, CA) and pooled them to achieve an equimolar concentration of each index-tagged sample, resulting in a final concentration of 4 nM, including the PhiX Control Library. The pooled samples underwent cluster generation and were sequenced on the MiSeq platform (Illumina, San Diego, CA) using a 2×250 paired-end format. We conducted metagenomic analysis using QIIME2 [70], version 2023–5.1. The 16S rDNA V3–V4 region amplicons paired-end sequence data was imported into the qiime2 program. We merged the reads using “vsearch” and quality filtered. De-noising and quality control were performed with “Deblur denoise-16S.” The qiime2 command “Features-table filter-features” was used to remove features appearing in only one sample and below 1% [70]. Taxonomy was assigned to OTUs by using the sklearn method and aligning against the SILVA138.1 database, downloaded from the SILVA website [71]. To calculate the alpha and beta diversity, we used “qiime phylogeny” and “qiime diversity core-metrics-phylogenetic” commands. The “qiime diversity alpha-rarefaction” command was used to obtain the alpha-rarefaction curves. We used the package “ape” [72] in the software R (v 4.1.2; <https://www.R-project.org/>) and Graph Pad Prism 10.0 (Graphpad software), to plot graph and for statistical analysis, respectively.

Statistical analyses

We analysed fitness and physiological data using Graph-Pad Prism 8.0.1. We checked whether datasets conformed to a normal distribution using the Shapiro–Wilk test [59]. Data of HW-related mortality, hatching rate, larval developmental time, pupal developmental time, larval viability, pupal viability, sex ratio, fecundity, fertility, blood feeding rate, trypsin activity and quantification of proteins in females offered a blood meal after HW exposure were normally distributed so we used a parametric two-way ANOVA, followed by a Tukey’s multiple comparison test for post-hoc analyses (Additional File 1: Tables S7–9) [73]. Energy reserve data did not follow normal distribution, so we assessed differences using a Kruskal–Wallis test followed by Dunn’s multiple comparison test (Additional File 1: Table S9) [59]. We compared the survival of HW-exposed mosquitoes through a Kaplan–Meier analysis and Mantel–Cox test [74].

Abbreviations

DEG Differentially expressed genes
GO Gene ontology

HSP Heat shock proteins
HW Heatwave
T_a Environmental temperature

Supplementary Information

The online version contains supplementary material available at <https://doi.org/10.1186/s12915-026-02567-x>.

Additional file 1. Nine supplementary tables supporting the results of the manuscript, including: Table S1. Larvae DEGs after a HW exposure; Table S2. Females’ and males’ DEG Lists A, B and C; Table S3. Percentage of bacterial OTUs in heatwave exposed and non-exposed larvae and adults. (a) Larvae pool samples. Female individuals of Crema (b) and Foshan (c) strain; Table S4. Scaled gene counts from individuals used for transcriptomic analyses; Table S5. Total number and percentages of expressed genes across life stages and treatments of *Ae. albopictus*; Table S6. GO enrichment of DEGs using different controls for considering 2 days time effect; Table S7. Statistic tests for significant differences in eggs and larvae fitness traits. (a) Egg hatching rate. (b) Larvae mortality. (c) Larval viability. (d) Pupal viability. (e) Larval developmental time. (f) Pupal developmental time. (g) Sex ratio; Table S8. Statistic tests for significant differences in reproductive traits. (a) Fecundity and (b) fertility of HW-exposed males. Non-egg-laying females (c) and non-fertile females (d) crossed with HW-exposed males. (e) Bloodfeeding rate of HW-exposed females before blood meal (AHWb). (f) Fecundity and (g) fertility of HW-exposed females after a blood meal (AbHW). Non-egg laying (h) and non-fertile (i) AHWb. Fecundity (j) and fertility (k) of AbHW females. Non-egg laying (l) and non-fertile (m) AbHW females; Table S9. Statistic tests for significant differences in adult mortality and energy reserves. Female (a) and male (b) mortality. (c) Protein content. (d) Carbohydrate content. (e) Glycogen content. (f) Lipid content. (g) Protein compensation of HW-exposed sugar-fed females three days after bloodmeal. (h) Protein content of HW-exposed females after a blood meal (AbHW).

Additional file 2. Figure S1. Assessment of ovarian physiology after a HW. Ovaries stained with neutral red of sugarfed and bloodfed females of Crema (Cr) and Foshan (Fo) strain after the HW. The arrows indicate lysosomes present in the ovarian follicles.

Additional file 3. Figure S2. Transcriptome controls for considering the 2-day time effect of the HW in adults. (a) Simulated heatwave conditions and sampling points for the transcriptomic analyses of adults. The blue line on the graph shows the standard rearing conditions, and the red line represents the HW conditions. Females and males were exposed to HW at 6 days old and collected on day 9 (AsHW, red) together with their unexposed counterparts (As9, blue). To address the fact that HW lasts two days, we further sampled females and males on day 6 post emergence (As6, light blue). (b) We obtained the list of DEGs between As6 vs AsHW (red, A), As6 vs As9 (blue, B) and As9 vs AsHW (dark red, C). All genes of List A that are shared with List B were removed as we expect these genes to reflect differences in expression between mosquitoes sampled at 6 and 9 days post emergence, and the remaining DEGs of List A were compared to those of List C. We selected the List C for all the rest of the transcriptional analyses performed

Additional file 4. Figure S3. Genes that are expressed across life-stages of *Ae. albopictus* after experiencing a HW. (a) Principal component analysis using the normalized counts of all samples. Triangles represent larvae, dots females and square males. Red and blue refer to samples exposed to a HW or kept at standard rearing conditions, respectively. (b) Linear regressions of DEGs lists when using Log₂FC values of 1, 1.5 and 2, of larvae, females and males. For adults, the linear regressions are plotted for List A (light blue), List B (blue) and List C (red) of DEGs. The correlation coefficient is shown next to each line.

Acknowledgements

We are grateful to all members of the Bonizzoni’s lab for fruitful discussion.

Authors' contributions

CA performed biological experiments, contributed to bioinformatic analysis of transcriptomic data, analyzed the data and wrote the manuscript; ANLC contributed to bioinformatic analyses of transcriptomic data, statistical analyses of all data, and analyzed the data; AK1 contributed to energy reserve experiments and analyzed the data; AK2 contributed to overall data analysis. PLC performed bioinformatic analyses of microbiota data; AC analysed the microbiota data; CD analysed the microbiota data; GF contributed to microbiota analysis and contributed with funding; MB conceived and supervised the study, obtained funding and wrote the manuscript with feedback from all authors. All authors read and approved the final manuscript.

Funding

The authors would like to thank the following for their financial support of research: Ministero dell'Università e della Ricerca, Italia (Research Grant number 2022J45MLL) to Bonizzoni M. and Favia G. and EU funding within the NextGeneration EU-MUR PNRR Extended Partnership initiative on Emerging Infectious Diseases (Project no. PE00000007, INF-ACT) to M. Bonizzoni.

Data availability

Whole Genome Sequencing data that support the findings of this study are openly available in NIH SRA BioProject ID number PRJNA1272515 [75]. All raw scaled reads data counts per sample generated by our research, as well as the command lined used to run nf-core/RNAseq and a custom R script used to estimate DEGs using DESeq2 for the transcriptomic analysis were deposited in a publicly accessible repository [76].

Declarations

Ethics approval and consent to participate

Not applicable.

Consent for publication

Not applicable.

Competing interests

The authors declare no competing interests.

Received: 29 July 2025 Accepted: 20 February 2026

Published online: 26 February 2026

References

- Mirth CK, Saunders TE, Amourda C. Growing up in a changing world: environmental regulation of development in insects. *Annu Rev Entomol.* 2021;66:81–99.
- Meehl GA, Tebaldi C. More intense HW due to climate change. *Science.* 2004;305:994–8.
- Hendrix DL, Salvucci ME. Polyol metabolism in homopterans at high temperatures: accumulation of mannitol in aphids (Aphididae: Homoptera) and sorbitol in whiteflies (Aleyrodidae: Homoptera). *Comparative Biochemistry and Physiology Part A: Molecular & Integrative Physiology.* 1998;120:487–94.
- Lahondère C. Recent advances in insect thermoregulation. *J Exp Biol.* 2023;226:jeb.245751. <https://doi.org/10.1242/jeb.245751>.
- Nguyen TTA, Michaud D, Cloutier C. A proteomic analysis of the aphid *Macrosiphum euphorbiae* under heat and radiation stress. *Insect Biochem Mol Biol.* 2009;39:20–30.
- González-Tokman D, Córdoba-Aguilar A, Dáttilo W, et al. Insect responses to heat: physiological mechanisms, evolution and ecological implications in a warming world. *Biol Rev.* 2020;95:802–21.
- Clissold FJ, Simpson SJ. Temperature, food quality and life history traits of herbivorous insects. *Curr Opin Insect Sci.* 2015;11:63–70.
- Colinet H, Sinclair BJ, Vernon P, et al. Insects in fluctuating thermal environments. *Annu Rev Entomol.* 2015;60:123–40.
- Walsh BS, Parratt SR, Hoffmann AA, et al. The impact of climate change on fertility. *Trends Ecol Evol.* 2019;34:249–59.
- Kingsolver JG, Arthur Woods H, Buckley LB, et al. Complex life cycles and the responses of insects to climate change. *Integr Comp Biol.* 2011;51:719–32.
- Pincebourde S, Casas J. Warming tolerance across insect ontogeny: influence of joint shifts in microclimates and thermal limits. *Ecol.* 2015;96:986–97.
- Ren L, Zhang X, Yang F, et al. Effects of heat tolerance on the gut microbiota of *Sarcophaga peregrina* (Diptera: Sarcophagidae) and impacts on the life history traits. *Parasit Vectors.* 2023;16:1–11.
- Sales K, Vasudeva R, Gage MJG. Fertility and mortality impacts of thermal stress from experimental heatwaves on different life stages and their recovery in a model insect. *R Soc Open Sci.* 2021;8(3):201717. <https://doi.org/10.1098/rsos.201717>.
- Zhao F, Hoffmann AA, Xing K, et al. Life stages of an aphid living under similar thermal conditions differ in thermal performance. *J Insect Physiol.* 2017;99:1–7.
- Zani PA, Cohnstaedt LW, Corbin D, et al. Reproductive value in a complex life cycle: Heat tolerance of the pitcher-plant mosquito. *Wyeomyia smithii* *J Evol Biol.* 2005;18:101–5.
- Li K, Gong Z. Feeling hot and cold: thermal sensation in *Drosophila*. *Neurosci Bull.* 2017;33:317–22.
- Achee NL, Grieco JP, Vandoost H, et al. Alternative strategies for mosquito-borne arbovirus control. *PLoS Negl Trop Dis.* 2019;13:1–22.
- Bonizzoni M, Gasperi G, Chen X, et al. The invasive mosquito species *Aedes albopictus*: current knowledge and future perspectives. *Trends Parasitol.* 2013;29:460–8.
- Farooq Z, Segelmark L, Rocklöv J, et al. Impact of climate and *Aedes albopictus* establishment on dengue and chikungunya outbreaks in Europe: a time-to-event analysis. *Lancet Planet Health.* 2025;9:e374–83.
- Bohers C, Vazeille M, Bernaoui L, et al. *Aedes albopictus* is a competent vector of five arboviruses affecting human health, greater Paris, France, 2023. *Euro Surveill.* 2024;29:1–7.
- Aranda C, Martínez MJ, Montalvo T, et al. Arbovirus surveillance: first dengue virus detection in local *aedes albopictus* mosquitoes in Europe, Catalonia, Spain, 2015. *Euro Surveill.* 2018;23(47):1700837. <https://doi.org/10.2807/1560-7917.ES.2018.23.47.1700837>.
- Carlassara M, Khorramnejad A, Oker H, et al. Population-specific responses to developmental temperature in the arboviral vector *Aedes albopictus*: Implications for climate change. *Glob Chang Biol.* 2024;30:1–22.
- World-Weather, <https://world-weather.info/forecast/italy/rome/august-2021/> (2021).
- Clifton ME, Noriega FG. Nutrient limitation results in juvenile hormone-mediated resorption of previtellogenic ovarian follicles in mosquitoes. *J Insect Physiol.* 2011;57:1274–81.
- Bai CM, Ma G, Cai WZ, et al. Independent and combined effects of daytime heat stress and night-time recovery determine thermal performance. *Biol Open.* 2019;26:bio038141. <https://doi.org/10.1242/bio.038141>.
- Zhu L, Wang L, Ma CS. Sporadic short temperature events cannot be neglected in predicting impacts of climate change on small insects. *J Insect Physiol.* 2019;112:48–56.
- Ma CS, Ma G, Pincebourde S. Survive a warming climate: insect responses to extreme high temperatures. *Annu Rev Entomol.* 2021;66:163–84.
- Peklanská M, van Heerwaarden B, Hoffmann AA, et al. Elevated developmental temperatures below the lethal limit reduce *Aedes aegypti* fertility. *J Exp Biol.* 2025. <https://doi.org/10.1242/JEB.249803>.
- Zhao L, Becnel JJ, Clark GG, et al. Expression of *aeaHsp26* and *aeaHsp83* in *Aedes aegypti* (Diptera: Culicidae) larvae and pupae in response to heat shock stress. *J Med Entomol.* 2010;47:367–75.
- Mack LK, Attardo GM. Heat shock proteins, thermotolerance, and insecticide resistance in mosquitoes. *Front Insect Sci.* 2024;4:1–7.
- Arrese EL, Soulages JL. Insect fat body: energy, metabolism, and regulation. *Annu Rev Entomol.* 2010;55:207–25.
- Ueda K, Imamura M, Saito A, et al. Purification and cDNA cloning of an insect defensin from larvae of the longicorn beetle. *Acalolepta luxuriosa* *Appl Entomol Zool.* 2005;40:335–45.
- Feder ME, Hofmann GE. Heat-shock proteins, molecular chaperones, and the stress response: evolutionary and ecological physiology. *Annu Rev Physiol.* 1999;61:243–82.

34. Taguwa S, Maringer K, Li X, et al. Defining Hsp70 subnetworks in Dengue virus replication reveals key vulnerability in Flavivirus infection. *Cell*. 2015;163:1108–23.
35. Taguwa S, Yeh MT, Rainbolt TK, et al. Zika virus dependence on host Hsp70 provides a protective strategy against infection and disease. *Cell Rep*. 2019;26:906–920.e3.
36. Sales K, Vasudeva R, Dickinson ME, et al. Experimental heatwaves compromise sperm function and cause transgenerational damage in a model insect. *Nat Commun*. 2018;9:1–11.
37. Rukke BA, Sivasubramaniam R, Birkemoe T, et al. Temperature stress deteriorates bed bug (*Cimex lectularius*) populations through decreased survival, fecundity and offspring success. *PLoS ONE*. 2018;13:1–16.
38. Rukke BA, Aak A, Edgar KS. Mortality, temporary sterilization, and maternal effects of sublethal heat in bed bugs. *PLoS One*. 2015;10:1–16.
39. David JR, Araripe LO, Chakir M, et al. Male sterility at extreme temperatures: a significant but neglected phenomenon for understanding *Drosophila* climatic adaptations. *J Evol Biol*. 2005;18:838–46.
40. Porcelli D, Gaston KJ, Butlin RK, et al. Local adaptation of reproductive performance during thermal stress. *J Evol Biol*. 2017;30:422–9.
41. Zheng J, Cheng X, Hoffmann AA, et al. Are adult life history traits in oriental fruit moth affected by a mild pupal heat stress? *J Insect Physiol*. 2017;102:36–41.
42. Roux O, Le Lann C, Van Alphen JJM, et al. How does heat shock affect the life history traits of adults and progeny of the aphid parasitoid *Aphidius avenae* (Hymenoptera: Aphididae)? *Bull Entomol Res*. 2010;100:543–9.
43. Time & Date, www.timeanddate.com/weather/italy/rome/historic?month=8&year=2024 (2024).
44. Malook S, Arora AK, Wong ACN. The role of microbiomes in shaping insecticide resistance: current insights and emerging paradigms. *Curr Opin Insect Sci*. 2025;69:1–11.
45. Black WC, Alphey L, James AA. Why RIDL is not SIT. *Trends Parasitol*. 2011;27(8):362–70. <https://doi.org/10.1016/j.pt.2011.04.004>.
46. Cator LJ, Wyer CAS, Harrington LC. Mosquito sexual selection and reproductive control programs. *Trends Parasitol*. 2021;37:330–9.
47. Ross PA, Wiwatanaratnabutr I, Axford JK, et al. *Wolbachia* infections in *Aedes aegypti* differ markedly in their response to cyclical heat stress. *PLoS Pathog*. 2017;13:1–17.
48. Mancini MV, Herd CS, Ant TH, et al. *Wolbachia* strain wAu efficiently blocks arbovirus transmission in *Aedes albopictus*. *PLoS Negl Trop Dis*. 2020;14:1–15.
49. Palatini U, Masri RA, Cosme LV, et al. Improved reference genome of the arboviral vector *Aedes albopictus*. *Genome Biol*. 2020;21:1–29.
50. Tsujimoto H, Adelman ZN. Improved fecundity and fertility assay for *Aedes aegypti* using 24 well tissue culture plates (Eagal plates). *J Vis Exp*. 2021;4:171. <https://doi.org/10.3791/61232>.
51. Gulia-Nuss M, Eum JH, Strand MR, et al. Ovary ecdysteroidogenic hormone activates egg maturation in the mosquito *Georgacraigius atropalpus* after adult eclosion or a blood meal. *J Exp Biol*. 2012;215:3758–67.
52. Clifton ME, Noriega FG. The fate of follicles after a blood meal is dependent on previtellogenic nutrition and juvenile hormone in *Aedes aegypti*. *J Insect Physiol*. 2012;58:1007–19.
53. Patel H, Manning J, Ewels P, et al. nf-core/rnaseq: nf-core/rnaseq v3 19.0. Tungsten Turtle. Zenodo. 2025. <https://doi.org/10.5281/zenodo.15631172>.
54. van Gorp T, McIntyre L, Verhoeven K. Consistent errors in first strand cDNA due to random hexamer mispriming. *PLoS ONE*. 2013;30(8):e85583.
55. Patro R, Duggal G, Love M, et al. Salmon provides fast and bias-aware quantification of transcript expression. *Nat Methods*. 2017;14:417–9.
56. Love MI, Huber W, Anders S. Moderated estimation of fold change and dispersion for RNA-seq data with DESeq2. *Genome Biol*. 2014;15:1–21.
57. Heberle H, Meirelles GV, da Silva FR, et al. InteractiVenn: a web-based tool for the analysis of sets through Venn diagrams. *BMC Bioinformatics*. 2015. <https://doi.org/10.1186/s12859-015-0611-3>.
58. Blighe K, Rana S, Lewis M. EnhancedVolcano: Publication-ready volcano plots with enhanced colouring and labeling. Epub ahead of print 2025. <https://doi.org/10.18129/B9.bioc.EnhancedVolcano>.
59. Ramachandran KM, Tsokos CP. *Mathematical Statistics with Applications*. London: Academic Press; 2020.
60. Lozada-Chávez AN, Lozada-Chávez I, Alfano N, et al. Adaptive genomic signatures of globally invasive populations of the yellow fever mosquito *Aedes aegypti*. *Nat Ecol Evol*. 2025;9:652–71. <https://doi.org/10.1038/s41559-025-02643-5>.
61. Götz S, García-Gómez JM, Terol J, et al. High-throughput functional annotation and data mining with the Blast2GO suite. *Nucleic Acids Res*. 2008;36:3420–35.
62. O’Leary NA, Wright MW, Brister JR, et al. Reference sequence (RefSeq) database at NCBI: current status, taxonomic expansion, and functional annotation. *Nucleic Acids Res*. 2016;44:D733–45.
63. Jones P, Binns D, Chang HY, et al. InterProScan 5: genome-scale protein function classification. *Bioinformatics*. 2014;30:1236–40.
64. Mistry J, Chuguransky S, Williams L, et al. Pfam: The protein families database in 2021. *Nucleic Acids Res*. 2021;49:D412–9.
65. Sigrist CJ, De Castro E, Cerutti L, et al. New and continuing developments at PROSITE. *Nucleic Acids Res*. 2013;41:344–7.
66. Wilson D, Pethica R, Zhou Y, et al. SUPERFAMILY - Sophisticated comparative genomics, data mining, visualization and phylogeny. *Nucleic Acids Res*. 2009;37:380–6.
67. Haft DH, Selengut JD, White O. The TIGRFAMs database of protein families. *Nucleic Acids Res*. 2003;31:371–3.
68. Wu T, Hu E, Xu S, et al. clusterProfiler 4.0: a universal enrichment tool for interpreting omics data. *The Innovation*. 2021;2:100141.
69. Klindworth A, Pruesse E, Schweer T, et al. Evaluation of general 16S ribosomal RNA gene PCR primers for classical and next-generation sequencing-based diversity studies. *Nucleic Acids Res*. 2013;41:1–11.
70. Boley E, Rideout JR, Dillon MR, et al. Reproducible, interactive, scalable and extensible microbiome data science using QIIME 2. *Nat Biotechnol*. 2019;37:852–7.
71. Quast C, Pruesse E, Yilmaz P, et al. The SILVA ribosomal RNA gene database project: Improved data processing and web-based tools. *Nucleic Acids Res*. 2013;41:590–6.
72. Paradis E, Schliep K. Ape 5.0: an environment for modern phylogenetics and evolutionary analyses in R. *Bioinformatics*. 2019;35:526–8.
73. Lee S, Lee DK. What is the proper way to apply the multiple comparison test? *Korean J Anesthesiol*. 2018;71:353–60.
74. Goel M, Khanna P, Kishore J. Understanding survival analysis: Kaplan-meier estimate. *Int J Ayurveda Res*. 2010;1:274.
75. Alfaro C, Lozada-Chávez AN, Khorramnejad A, et al. Assessing transcriptional changes in *Aedes albopictus* following a heatwave. *NCBI BioProject*. <https://identifiers.org/bioproject:PRJNA1272515> (2026)
76. Alfaro C, Lozada-Chávez AN, Khorramnejad A, et al. *Aedes albopictus* responses to a heatwave. *Zenodo*. <https://doi.org/10.5281/zenodo.18274507> (2026)

Publisher’s Note

Springer Nature remains neutral with regard to jurisdictional claims in published maps and institutional affiliations.